Spontaneous Curvature of Comblike Polymers at a Flat Interface

Igor I. Potemkin,*,† Alexei R. Khokhlov,† Svetlana Prokhorova,‡ Sergei S. Sheiko,*,§ Martin Möller,⊥ Kathryn L. Beers,∥ and Krzysztof Matyjaszewski∥

Physics Department, Moscow State University, Moscow, 119992 Russia, Institute for Microsystem Technology, University of Freiburg, Georges-Koehler-Allee 103, D-79110 Freiburg, Germany, Department of Chemistry, University of North Carolina at Chapel Hill, North Carolina, 27599-3290, Institut fuer Technische Chemie und Makromolekulare Chemie, RWTH Aachen, D-52062 Aachen, Germany, and Department of Chemistry, Carnegie Mellon University, 4400 Fifth Avenue, Pittsburgh, Pennsylvania 15213

Received September 23, 2002; Revised Manuscript Received February 17, 2004

ABSTRACT: Spontaneous curvature of molecular brushes adsorbed on a flat substrate was observed by scanning force microscopy for comblike polymers of poly(butyl acrylate). This phenomenon was analyzed theoretically for a 2D model of a brush molecule in the regime of strong adsorption. Although all side chains were confined to the substrate plane, they were allowed to flip over and change their position with respect to the backbone. Instability of the straight backbone was caused solely by the entropic elasticity of the side chains: smaller extension of the side chains was attained upon their uneven distribution relative to the backbone. An equilibrium, i.e., spontaneous, curvature resulted from competition between elasticity of the side chains and stabilizing factors such as inherent stiffness of the backbone, mixing entropy of the side chains and excluded volume interactions of distant parts of the brush. The curvature radius is found to be proportional to the degree of polymerization of the side chains. The effect of polydispersity of the side chains is discussed.

1. Introduction

Cylindrical brush molecules, sometimes called bottle brushes, are polymer molecules which consist of a long flexible main chain (backbone) and densely grafted side chains.[1−5] The interest in such molecules is due to conformational effects caused by competition of the flexibility of the backbone and the flexibility of the side chains. So far, much theoretical attention has been focused on the study of cylindrical brushes in solution.[6−10] The main objective of the experimental studies was to verify the hypothesis about lyotropic ordering in such a system due to enhanced stiffness of the brush molecules.[2] The other objective was to measure the axial contraction of the main chain as a function of the side chain length and the solvent quality.[11−14]

Experimental and theoretical studies of cylindrical brushes adsorbed on a flat surface raised additional interest in this system.[14−18] Recently, we have observed transition between two conformations of cylindrical brush molecules tightly adsorbed to a flat interface.[18] The first-order phase transition from a rodlike to a globular conformation was observed upon compression of a monolayer of poly(*n*-butyl acrylate) (PBA) brushes on a water surface. In their original state (as adsorbed), molecules in a dense monolayer adopt an extended conformation (Figure 1a). Upon compression and subsequent expansion of the monolayer, the molecules undergo a transition to a curved conformation (Figure 1b). The peculiar feature of the curved conformation is that the curvature is the same throughout the entire mol-

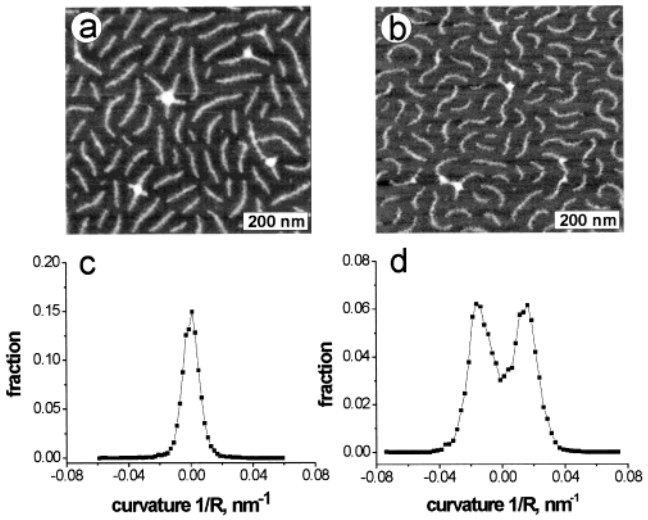

Figure 1. (a) Molecular structure of a dense monolayer of PBA brushes (with $N = 567$, $M = 57$) adsorbed on a surface of water and transferred to a mica substrate for AFM observations. The molecules are fully extended. The white threads correspond to backbone, while the area between the threads is covered by adsorbed side chains. (b) Molecular structure of the same monolayer after 3-fold compression and subsequent expansion. The molecules became curved and the curvature is fairly constant. (c and d) Curvature distribution functions of the brushes presented in images a and b, respectively. These functions were measured for a large ensemble of molecules (ca. 2000 species) using custom software.

* To whom correspondence should be addressed.E-mail: (I.I.P.) igor@polly.phys.msu.ru; (S.S.S.) sergei@email.unc.edu.
† Moscow State University.
‡ University of Freiburg.
§ University of North Carolina at Chapel Hill.
⊥ RWTH Aachen.
∥ Carnegie Mellon University.

10.1021/ma021519d CCC: $27.50
Published on Web 04/20/2004

ecule. Preliminary analysis of the molecular conformation including the coexistence of the straight and curved conformations is reported in ref 19. In this paper, we give a theoretical explanation to the observed phenomenon (spontaneous curvature).

Theoretical analysis of the experimental results[18] showed that the conformation of the adsorbed brush molecules depends on the fraction of adsorbed side chains which is controlled by interactions of monomeric units with the substrate and by the entropic elasticity of the side chains. Moreover, distribution of the side chains between the two sides of the backbone can cause additional variations of the molecular conformation. Computer simulations[15] and theoretical analysis[17] showed that spiral conformations are expected if the side chains are unevenly distributed with respect to the backbone.

In the previous articles, the position of the side chains was fixed. Here we report on the equilibrium conformation of the adsorbed brush molecules whose side chains were allowed to flip over relative to the backbone. The most remarkable observation is that elasticity of the side chains alone can cause instability of the straight conformation of the backbone and cause its bending. A similar kind of instability was predicted in ref 20 for the case of planar polymer bilayers. On the basis of a scaling approach the authors have shown that redistribution of the polymer chains from inner to outer layers reduces the free energy of the system and stabilizes spherically bent configuration of the membrane while the membrane remains stable toward bending into a cylinder. In this article, we will show that spontaneous bending of a 2D comb, which corresponds to the bending of the bilayer into a cylinder, can occur.

2. Experimental Section

Cylindrical brushes with PBA side chains and polymethacrylate backbone were prepared as described elsewhere.[3,18,21−23] The lengths of the backbone and of the side chains were characterized using a combination of AFM and GPC with a multiangle laser light scattering (MALLS) detector. The degree of polymerization of the backbone was measured to be $N = 567 \pm 40$, while the degree of polymerization of the PBA side chains were determined as $M = 57 \pm 5$.

Monolayers were prepared using a symmetric compression trough (KSV-5000, KSV Instruments) filled with double-distilled water (Milli-Q). Even spreading of the brush molecules was achieved by deposition of small 10 μL portions of a dilute solution of brushes in chloroform ($c = 1$ mg/mL) on the water surface and subsequent compression by two barriers at a speed of 50 cm^2/min. The compression was performed at a 30 min delay after deposition to favor equilibration of the film structure. Monolayers were transferred onto a mica substrate for SFM measurements at a transfer speed of 0.5 mm/min. During the film transfer, the pressure was maintained constant at $\pi = 1$ mN/m via concurrent motion of the barriers. The transfer ratio (the ratio between the area of the transferred film and the displacement of the barrier during the transfer) was measured to be 0.996.

Tapping mode AFM (Nanoscope IIIa, Digital Instruments, Santa Barbara, CA) was used to obtain molecular resolution of the transferred monolayers. The measurements were performed at ambient conditions (in air, 56% relative humidity, 27 °C) using Si cantilevers with a spring constant of ≈50 N/m and a resonance frequency of about 300 kHz. The set-point amplitude ratio was maintained at 0.9 to minimize the sample deformation due to the mechanical contact with the tip.

Experimental Results. Equilibration of tightly adsorbed brush molecules is prohibited by the interaction with the substrate. Once adsorbed on a mica substrate, the brush molecules do not change their conformation due to relatively high molecular weight and due to strong interaction with the substrate. To facilitate equilibration, poly(butyl acrylate) brushes were adsorbed on a surface of water and subjected to a series of compression−decompression cycles. Owing to the amphiphilic nature of *n*-butyl acrylate groups, the brushes spread readily on the water surface. Similar to other fluids, compression of the PBA brushes was reversible as expected for equilibrium spreading. To visualize the conformation of individual molecules, monolayers were transferred to a mica substrate and imaged by SFM. Figure 1a shows a tapping mode micrograph (height contrast) obtained from the polymer before compression. Brush molecules were resolved as individual wormlike particles lying parallel to the substrate plane. The white threads correspond to the backbone embedded into a shell of desorbed side chains, whereas the area between the threads is covered by adsorbed side chains. The molecules lie flat on mica substrate due to strong interaction between the side chains and the substrate. The side chains also determine the distance between the molecules. It was shown that the distance is proportional to the number-average length of the side chains.[18] This observation is consistent with the nearly complete (2D) adsorption of high fraction of the PBA side chains.

Compression of the brush monolayer results in desorption of the side chains and their aggregation around the backbone. It can cause conformational transition from the rodlike to a globular conformation.[18] The subsequent expansion of the monolayer leads to readsorption of the side chains and thus extension of the backbone. During adsorption, the side chains can deliberately choose their position with respect to the backbone to minimize the total free energy. Therefore, a series of compression−expansion cycles should favor equilibration of the backbone conformation. SFM micrographs of the monolayer after decompression up to initial value (1 mN/m) is depicted in Figure 1b. This state is characterized by the same temperature and surface area of the monolayer as the state before compression, Figure 1a. One can see that many molecules are curved and demonstrate the characteristic C- or S-like conformations. The most striking observation is that the adsorbed molecules have a similar curvature. Figure 1d depicts the curvature distribution showing two equally spaced bands of positive and negative curvatures that correspond to the clockwise and counterclockwise bends of the molecular contour in the surface plane. This indicates a preferred curvature of surface confined cylindrical brush molecules. In contrast, the brushes before compression (Figure 1a) demonstrate a typical Gaussian distribution with one peak at zero curvature, Figure 1c.

As mentioned above, equilibration of large polymer molecules is prohibitively slow due to strong interaction of the side chains with the substrate (k_BT per monomeric unit). Although the mechanically induced desorption-readsorption cycles favor the equilibration process, kinetics largely control the final conformation. Therefore, a series of experiments were carried out to verify the equilibrium. In these experiments, (i) the adsorption was performed both from melt and from dilute solution to vary the starting conformation, (ii) in addition to the compression experiments, the desorption−readsorption of side chains was also induced by periodic variation of the surface energy of the substrate, and (iii) we observed the transition from the straight to curved conformations upon annealing of adsorbed molecules in appropriate solvents. The curvature distribution function in all mentioned experiments reveals two equally spaced peaks. Therefore, we believe that the curved conformation of adsorbed brush molecules corresponds to the equilibrium one. The experimental studies will be reported elsewhere. Here, we present theoretical explanation of the spontaneous curvature.

3. Model and Free Energy of Adsorbed Comblike Polymer

To analyze possible conformations of *strongly adsorbed* brush molecules we consider a 2D model of the

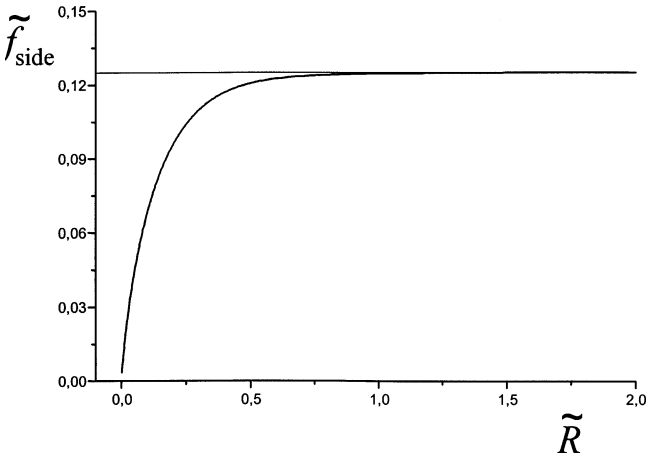

Figure 2. Elastic free energy of the side chains $\tilde{f}_{side} = f_{side}\lambda_s/M$ as a function of the curvature radius $\tilde{R} = R/aM = 1/(6z)$ which is obtained after minimization of a sum of eqs 5 and 6 with respect to β. The horizontal line depicts the free energy of the unbent brush with $R = \infty$ and $\beta = {}^1/_2$.

comblike polymers in a monolayer in which the left−right location of the side chains with respect to the backbone is *not fixed* but determined by the condition of thermodynamic stability (minimum free energy) of the molecule. Polymer molecules are considered to be incompatible with the surrounding medium, i.e., when attractive forces dominate between monomer units of the side chains and the backbone. Minimization of the polymer−solvent contact area results in dense packing of monomer units in the monolayer which can be considered as a 2D melt. N and M denote the numbers of monomer units in the backbone and side chains, respectively, $N \gg M \gg 1$; a is their linear size. We consider densely grafted polymer brushes, i.e., side chains are attached to each monomer unit of the backbone and their number is equal to N.

Local excess of the side chains at one side of the backbone can induce bending of the brush molecule.[15,17] To find the free energy of the brush molecule per unit length we divide the brush in sections containing dN monomer units in the backbone where dN_1 (left) and dN_2 (right) side chains form convex and concave sides of the section, respectively, $dN \gg 1$, $dN_1 > dN_2$, $dN_1 + dN_2 = dN$.

The free energy of the brush molecule per unit of its length in a dense monolayer comprises the elastic energies of the side chains and the backbone as well as the mixing entropy of the side chains

$$f = f_{left} + f_{right} + f_{bb} + f_{mix} \tag{1}$$

Note that the interfacial energy contribution to the free energy of the monolayer is constant (total surface area of the monolayer remains constant) and can be omitted in further considerations.

Let us denote as R the radius of the curvature of the brush (backbone) section, Figure 3b. The elastic free energy of the side chains forming the convex side of the brush section can be written as[17]

$$\frac{d\mathcal{F}_{left}}{k_B T} = \frac{dN_1}{2\lambda_s}\int_R^{R_1} dr\, E(r) \tag{2}$$

where λ_s is the Kuhn segment length of the side chains which are assumed to be flexible, $\lambda_s \ll aM$. Local

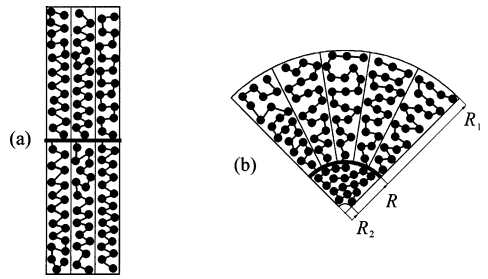

Figure 3. Schematic representation of symmetric (3 × 3, a) and asymmetric (5 × 1, b) distribution of the side chains (beads on filament) with respect to the backbone (bold line) in the brush section. Rectangular (a) and circular (b) regions, occupied by the side chains, have the same area. Arrows show the radii of the curvature of the backbone (R), and the boundaries of the side chain location at convex (R_1) and concave (R_2) sides.

stretching of the side chain $E(r) = dr/ds$ (derivative of the distance between two points of the chain with respect to the contour length between them) depends on the radial coordinate r, $R < r < R_1$. Here R_1 is the coordinate of free ends of the side chains which are assumed to be located at the same distance from the backbone (Alexander approximation for planar brushes[24]). The dense packing condition for the side chains in a circular sector of angle $d\varphi$, which is formed by a section of the brush of length $a\, dN = R\, d\varphi$, takes the form

$$r\, dr\, d\varphi = a\, ds\, dN_1 \tag{3}$$

Here ds is the contour length of the chain located in a ring layer with the width dr. Let us denote by $\beta = dN_1/dN$ the fraction of the side chains forming the convex side of the brush section. Using eq 3, we can find the following expressions for the local stretching of the chain

$$E(r) = \frac{dr}{ds} = \frac{a}{r}\frac{dN_1}{d\varphi} = \frac{\beta R}{r} \tag{4}$$

Substitution of eq 4 into eq 2 gives the following elastic energy of the side chains f_{left} per unit of length $dN\, a$ of the brush

$$f_{left} = \frac{d\mathcal{F}_{left}}{dN\, ak_B T} = \frac{\beta^2 R}{2\lambda_s a}\ln\left(\frac{R_1}{R}\right) = \frac{\beta^2 R}{4\lambda_s a}\ln\left(1 + \frac{2aM\beta}{R}\right) \tag{5}$$

where we used the condition $R_1^2 - R^2 = 2a^2M\, dN_1/d\varphi = 2aRM\beta$ obtained by integration of eq 3.

The expression for the free energy of the side chains forming the concave side of the brush can be derived in a similar way. The result is

$$f_{right} = -\frac{(1-\beta)^2 R}{4\lambda_s a}\ln\left(1 - \frac{2aM(1-\beta)}{R}\right) \tag{6}$$

The total elastic free energy of the side chains $f_{side} = f_{left} + f_{right}$ demonstrates instability of the brush molecule ($\beta = {}^1/_2$) with respect to its bending enabled by the side chain redistribution ($\beta \neq {}^1/_2$). To demonstrate this effect, let us expand f_{side} in a series in powers of

small dimensionless curvature $z = aM/(6R) \ll 1$ and small excess of the side chains $\epsilon = \beta - {}^1/_2 \ll 1$

$$f_{side} = \frac{M}{\lambda_s}\left(\frac{1}{8} + \frac{3}{2}(\epsilon - z)^2 - 12z\epsilon^3 + 60z^2\epsilon^2 - 81z^3\epsilon + \frac{162}{5}z^4 + ...\right) \quad (7)$$

where the first term in the brackets corresponds to the elastic energy of the unbent brush and the next terms are small corrections due to bending. Minimization of eq 7 with respect to ϵ at a fixed value of z yields

$$f_{side} = \frac{M}{\lambda_s}\left(\frac{1}{8} - \frac{3}{5}z^4 + ...\right), \quad \epsilon \approx z \quad (8)$$

One can see that small bending with redistribution of the side chains results in a decrease of the elastic energy of the side chains compared to the energy of the unbent symmetric brush. In the general case of arbitrary values of the curvature and fraction of the side chains f_{side} is always positive (see eqs 5 and 6) and attains its minimum, which is equal to zero, at $R \to 0$ and $\beta \to 1$, Figure 2. It means that an asymmetrical distribution of the side chains relative to the backbone, accompanied by the backbone bending, is more favorable than their symmetrical left−right distribution.

This effect has a clear physical explanation: In the case of a symmetrical brush each chain is confined by a rectangular area that results in strong elongation of the chain (the end-to-end distance has linear dependence on M), Figure 3a. The side chain of the asymmetrical brush occupies a circular sector of the same area, Figure 3b. In the convex side of the brush a width of this area increases from the backbone region to the region of free end of the chain. As a result, the local chain stretching falls away from the backbone and leads to a reduction of total elastic energy of the chain. The stretching of the chain on the concave side of the brush reduces too because of decreasing number of the chains, Figure 3b. Therefore, spontaneous curvature formation in each section of the brush is driven by elasticity of the side chains.

Figure 2 shows also that the elasticity of the side chains by itself can not stabilize the curvature of the comb (f_{side} has minimum at $R = 0$). We will show below that excluded volume interactions of distant parts of the 2D brush molecule (topological restrictions on the chain conformation) determine the curvature radius.

The third term in eq 1 is the elastic energy of the backbone. This contribution plays the role of a stabilizing factor, limiting the backbone bending. Note that *entropic* elastic energy of the backbone elongation is M times smaller ($M \gg 1$) than the elastic energy of the side chains and can be neglected. However the dense grafting of the side chains induces bending of the backbone on the length scales smaller than the persistence length of nongrafted backbone λ_b, $\lambda_b \geq a$. Therefore, the *bending* elasticity of the backbone should be taken into account. The corresponding free energy per unit length of the backbone is similar to that of an elastic rod with a bending modulus $k_BT\lambda_b$. At small curvature this energy has the form[25]

$$f_{bb} = \frac{\lambda_b}{2R^2} \quad (9)$$

The last term in eq 1 is the mixing entropy of the side chains. It is a combinatorial contribution accounting for a number of possible ways to create certain left−right distribution of the side chains with respect to the backbone:

$$f_{mix} = \frac{1}{a}[\beta \ln\beta + (1 - \beta)\ln(1 - \beta)] \quad (10)$$

This term also plays a role of the stabilizing factor and attains its minimum at $\beta = {}^1/_2$.

Thus, the total free energy of the brush f per unit length (local free energy) as a function of the curvature radius R and the fraction β of the side chains forming convex side of the brush, ${}^1/_2 \leq \beta \leq 1$, is given by the sum of eqs 5, 6, 9, and 10.

4. Results and Discussions

4.1. Equilibrium Conformations of the Brush Molecule. If we assume that the brush molecule attains its equilibrium state, it means that the total free energy of the brush molecule should have a minimum as a function of β and R for each fragment of the brush. Let us consider small bending of each fragment of the brush which is accompanied by equilibrium left−right distribution of the side chains. In this case interactions of the distant parts of the molecule do not influence on the curvature radius. The total free energy of small bending of the brush per unit length as a function of the curvature z takes the form

$$\Delta f = f - \left[\frac{M}{8\lambda_s} - \frac{\ln 2}{a}\right] = z^2\left(\frac{2}{a} + \frac{18\lambda_b}{a^2M^2}\right) - \frac{3M}{5\lambda_s}z^4 + ... \quad (11)$$

after minimization of the expanded free energy f, eq 1, with respect to ϵ, $\epsilon \approx z$. The expression in the square brackets corresponds to the energy of the unbent brush. The first term in the right-hand side of eq 11 comes from the expansion of the mixing entropy, eq 10, $f_{mix} = -\ln 2/a + 2\epsilon^2/a + ...$ The second term is the bending energy of the backbone and the third term corresponds to the decrease of the elastic energy of the side chains (see eq 8).

If the coefficient in parentheses of eq 11 is smaller than M/λ_s, $2/a + 18\lambda_b/a^2M^2 \ll M/\lambda_s$, i.e., the backbone is flexible enough, then the bending energy Δf can become negative at small values of z (solid part of curve a in Figure 4):

$$\frac{5\lambda_s}{3aM}\left(2 + \frac{18\lambda_b}{aM^2}\right) < z^2 \ll 1 \quad (12)$$

It means that in this regime the bending elasticity of the backbone and mixing entropy of the side chains are not able to stabilize rectilinear conformation of the brush which then becomes bent. More detailed analysis of eq 1 for arbitrary values of the curvature shows that these factors are not able to stabilize the curvature as well. The curvature is determined by topological confinements of the chain conformation (dotted part of curve a in Figure 4). Taking into account that the curvature radius cannot be smaller than the width of the concave side of the molecule (the end-to-end distance of the side chains) D, $D = R - R\sqrt{1-2aM(1-\beta)/R}$ (see Figure 5), we can define the optimum curvature radius

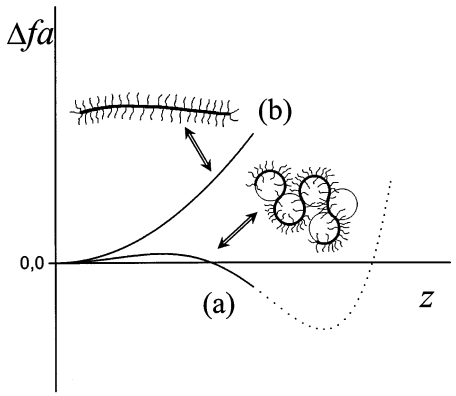

Figure 4. Characteristic dependences of the bending free energy of the brush Δfa on the curvature z for different values of the persistence length of the backbone (or side chain length): stability of bent (a) and rectilinear (b) shape of the brush segment at small and high values of λ_b, respectively.

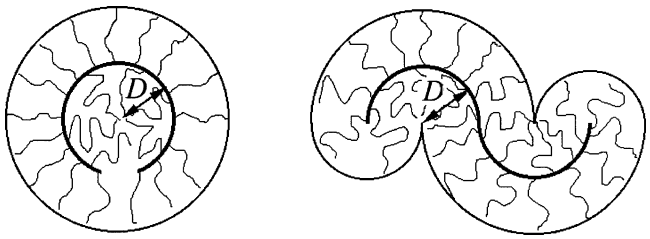

Figure 5. Schematic representation of C- and S-like conformations of the brush molecule with optimum curvature.

as $R \approx D$, i.e., as a minimum possible value. It gives $R \approx 2aM(1 - \beta)$. Because $1 - \beta$ is on the order of unity, we obtain the curvature radius scaling with the length of the side chains as $R \sim M$. This prediction is consistent with recent experimental data.[19] It has to be noted that in the considered case of minimum curvature radius, when according to the model all ends of the side chains of the concave side of the brush should be placed at thesame point, Figure 5, the elastic free energy, eq 6, has logarithmic divergency. This is a result of Alexander's approximation[24] and such divergency can be removed by consideration of radial distribution of the chain ends similar to the case of cylindrical micelles.[26]

If the coefficient in parentheses of eq 11 has the same order of magnitude as M/λ_s or larger, $18\lambda_b\lambda_s/a^2 \geq M^3$, i.e., the backbone is very stiff, then the term $\sim z^4$ gives a small correction to the bending energy and Δf increases monotonically with z from the minimum value $\Delta f = 0$ at $z = 0$, Figure 4b. The absence of the second minimum at higher values of z, $z \sim 1$, can be obtained from the analysis of eq 1. Therefore, even left−right distribution of the side chains with respect to the backbone corresponds to the equilibrium state of the brush with short side chains or stiff backbone. In this case, each section of the brush possesses zero equilibrium curvature, and we may expect that the macroconformation of such a brush is similar to that of a persistent polymer chain. Depending on the ratio of the brush contour length, L, to its persistence length, λ_{pers}, the conformation may be varied between a rod like one (small contour lengths, $L \ll \lambda_{pers}$) and that of a 2D coil in the melt (at $L \gg \lambda_{pers}$).

4.2. Does Polydispersity of the Side Chains Change the Mechanism of Spontaneous Curvature Formation? In the experiments, we used PBA brushes that are polydisperse ($M_w/M_n \approx 1.2$ regarding the length of the side chains). At first glance one can imagine that the local bending of the backbone can occur even at *symmetrical* left−right distribution of the side chains when longer and shorter side chains are segregated around the backbone and form convex and concave sides of the brush, respectively. However, it can be shown that the *asymmetrical* distribution of the side chains corresponds to the lowest free energy of the brush molecule. For this purpose let us consider a simple model of bimodal size distribution of the side chains: brush contains only two kinds of side chains differing in the length, $M_1 < M_2$, $M_1 = 2M/(x + 1)$, $M_2 = 2Mx/(x + 1)$. Here $M = (M_1 + M_2)/2$ is the average number of monomer units and the coefficient $x = M_2/M_1 \geq 1$ is related to the polydispersity as $M_w/M_n = (x + 1)^2/(4x)$. The number of long and short side chains in the brush is assumed to be equal. Let us now compare the elastic free energies of the side chains corresponding to three states of the brush: when (i) both long and short side chains are distributed symmetrically with respect to the backbone (f_1), (ii) they are completely segregated (f_2), and (iii) long and short side chains are free to choose their location relative to the backbone at a small bending of the brush (f_3):

$$f_1 = \frac{M}{4\lambda_s}\frac{1}{x+1}\left(1 + \frac{x-1}{8}\right)$$

$$f_2 = \frac{M}{8\lambda_s(x+1)} y \ln\frac{y+x}{y-1}, \quad y = R\frac{x+1}{2aM} \qquad (13)$$

$$f_3 = \frac{M}{4\lambda_s}\frac{1}{x+1}\left(1 + \frac{x-1}{8} - \frac{3(x-1)(x+7)}{16(x+1)^2}z^2 + ...\right)$$

These expressions are obtained using the same model of the 2D brush as that for the monodisperse case (Alexander approach for location of the side chain ends, 2D dense packing condition for monomer units). The curvature radius of the symmetrical brush, whose long and short side chains are completely segregated, is obtained by minimization of f_2 with respect to y. The result is $y \sim 1$. It is seen in eq 13, that f_1 and f_2 are of the same order of magnitude and if the coefficient $x < 13$ (polydispersity < 3.8), then even symmetrical distribution of both short and long side chains is more favorable ($f_1 < f_2$).

f_3 in eq 13 is obtained via expansion of the free energy of the polydisperse brush with asymmetrical distribution of the side chains (see eq 15 in Appendix) in a series of powers of small dimensionless curvature $z = aM/(6R) \ll 1$ and a small excess of short ($\epsilon_1 = \beta_1 - {}^1/_4 \ll 1$) and long ($\epsilon_2 = \beta_2 - {}^1/_4 \ll 1$) side chains of the brush. Then this expression is minimized with respect to ϵ_1 and ϵ_2 giving

$$\epsilon_1 = \frac{7 - 3x}{8(x+1)}z$$

$$\epsilon_2 = \frac{x+2}{2(x+1)}z \qquad (14)$$

Negative correction $\sim z^2$ in the free energy f_3 means that bending with redistribution of both kinds of side chains lowers the free energy of the side chains. It is seen from eq 14 that if $x < {}^7/_3$, there is excess of both kinds of the chains on one side relative to the backbone. Otherwise, when $\epsilon_1 < 0$, long and short side chains are segregated. However, $\epsilon_2 > |\epsilon_1|$ for any values of polydispersity. It means that longer chains flip over relative to the backbone preferentially and give the main contribution

to the local asymmetry in the distribution of the side chains. Owing to inequalities $f_2 > f_1 > f_3$, we can conclude that polydispersity of the side chains does not prevent asymmetric left−right redistribution of the side chains, resulting in spontaneous curvature formation.

5. Concluding Remarks

In the present paper, spontaneous curvature formation in single molecules in monolayer has been visualized by scanning force microscopy for PBA comblike polymers adsorbed on a water surface. An explanation of such phenomenon was given on the basis of a 2D model of the polymer with flip-flop side chains.

It was shown that the length of the side chains (flexibility of the backbone) plays a crucial role. Depending on M and λ_b, two different types of molecular conformation were predicted theoretically. The polymer with short side chains (or high persistence length) was shown to have an equal fraction of the chains to the left and right sides of the backbone. On the other hand, for large values of M (or small values of λ_b), the equilibrium conformation corresponds to a local excess of the side chains at one side of the backbone and spontaneous curvature formation. The curvature radius has linear dependence on the side chain length.

We have shown that polydispersity of the side chains does not change the mechanism of the spontaneous curvature. In particular, segregation of long and short side chains relative to the backbone with equal fraction on left and right sides is less favorable than an asymmetrical distribution of them.

Bending modulus and possible conformations of single 2D comblike polymer with attracting rigid rod side chains symmetrically distributed with respect to the backbone were discussed in ref 27. It was shown that the strength of the side chain interactions is responsible for the curvature formation and determines the bending modulus scaling law. In our case of 2D melt of the brushes, it is assumed that the attractive interactions between monomer units dominate. On the other hand, if the side chains repeal each other and do not fill completely the surface, the problem can be examined in terms of densely packed 2D blobs, i.e., reduced to the considered case. Also the mean-field calculations for the brushes with binary repulsive interactions between monomer units confirmed the mechanism of the spontaneous curvature.[28] Therefore, the side chain length-dependent conformational behavior of the polymer with flexible side chains, which is discussed in this paper, is independent of interactions and determined by a competition of *entropic* and *bending* elasticity of the side chains and the backbone, respectively.

Acknowledgment. I.I.P. and S.S.S. acknowledge the contribution of Ekaterina Zhulina and Michael Rubinstein for clarification of the mentod used to determine the equilibrium curvature. The financial support of the Deutsche Forschungsgemeinschaft within the SFB 569, the VolkswagenStiftung (Federal Republic of Germany), and the Russian Foundation for Basic Research is gratefully acknowledged. S.S.S. thanks the National Science Foundation for financial support (Grant ECS-0103307).

Appendix

Free energy of the side chains in polydisperse brush (with bimodal size distribution) per unit length of the brush has a form

$$f_{pd} = \frac{(\beta_1+\beta_2)^2 R}{4\lambda_s a}\ln\left(1+\frac{2aM_1}{R}(\beta_1+\beta_2)\right) + \frac{\beta_2^2 R}{4\lambda_s a}\ln\frac{R+2a(M_1\beta_1+M_2\beta_2)}{R+2aM_1(\beta_1+\beta_2)} - \frac{(1-\beta_1-\beta_2)^2 R}{4\lambda_s a}\times \ln\left(1-\frac{2aM_1}{R}(1-\beta_1-\beta_2)\right) - \frac{(1/2-\beta_2)^2 R}{4\lambda_s a}\times \ln\frac{R-2a(M_1(1/2-\beta_1)+M_2(1/2-\beta_2))}{R-2aM_1(1-\beta_1-\beta_2)} \quad (15)$$

where M_1 and M_2 are the numbers of monomer units in the side chains, $M_1 \le M_2$; β_1 and β_2 are the fractions of short and long side chains on one side with respect to the backbone, respectively. The numbers of long and short side chains in the brush are assumed to be equal.

References and Notes

(1) Tsukahara, K.; Tsutsumi, Y.; Yamashita, Y.; Shimada, S. *Macromolecules* **1990**, *23*, 5201.
(2) Wintermantel, M.; Fischer, K.; Gerle, M.; Ries, R.; Schmidt, M.; Kajiwara, H.; Urakawa, H.; Wataoka, I. *Angew. Chem., Int. Ed. Engl.* **1995**, *34*, 1472.
(3) Beers, K. L.; Gaynor, S. G.; Matyjaszewski, K.; Sheiko, S. S.; Möller, M. *Macromolecules* **1998**, *31*, 9413.
(4) Schappacher, M.; Deffieux, A. *Macromolecules* **2000**, *33*, 7371.
(5) Cheng, G.; Böker, A.; Zhang, M.; Krausch, G.; Müller, A. H. E. *Macromolecules* **2001**, *34*, 6883.
(6) Birshtein, T. M.; Borisov, O. V.; Zhulina, E. B.; Khokhlov, A. R.; Yurasova, T. A. *Polym. Sci. USSR* **1987**, *29*, 1293.
(7) Fredrickson, G. H. *Macromolecules* **1993**, *26*, 2825.
(8) Rouault, Y.; Borisov, O. V. *Macromolecules* **1996**, *29*, 2605.
(9) Subbotin, A.; Saariaho, M.; Ikkala, O.; ten Brinke, G. *Macromolecules* **2000**, *33*, 3447.
(10) Saariaho, M.; Subbotin, A.; Ikkala, O.; ten Brinke, G. *Macromol. Rapid Commun.* **2000**, *21*, 110.
(11) Gerle, M.; Fischer, K.; Roos, S.; Müller, A. H. E.; Schmidt, M.; Sheiko, S. S.; Prokhorova, S. A.; Möller, M. *Macromolecules* **1999**, *32*, 2629.
(12) Terao, K.; Hokajo, T.; Nakamura, Y.; Norisuye, T. *Macromolecules* **1999**, *32*, 3690.
(13) Fisher, K.; Schmidt, M. *Macromol. Rapid Commun.* **2001**, *22*, 787.
(14) Sheiko, S. S.; Möller, M. *Chem. Rev.* **2001**, *101*, 4099.
(15) Khalatur, P.; Khokhlov, A. R.; Prokhorova, S. A.; Sheiko, S. S.; Möller, M.; Reineker, P.; Shirvaniants, D.; Starovoitova, N. *Eur. Phys. J. E* **2000**, *1*, 99.
(16) Prokhorova, S. A.; Sheiko, S. S.; Mourran, A.; Möller, M.; Beginn, U.; Zipp, G.; Ahn, C.-H.; Percec, V. *Langmuir* **2000**, *16*, 6862.
(17) Potemkin, I. I.; Khokhlov, A. R.; Reineker, P. *Eur. Phys. J. E* **2001**, *4*, 93.
(18) Sheiko, S. S.; Prokhorova, S. A.; Beers, K. L.; Matyjaszewski, K.; Potemkin, I. I.; Khokhlov, A. R.; Möller, M. *Macromolecules* **2001**, *34*, 8354.
(19) Sheiko, S. S.; da Silva, M.; Shirvaniants, D. G.; Rodrigues, C. A.; Beers, K.; Matyjaszewski, K.; Potemkin, I. I.; Möller, M. *Polym. Prepr. (Am. Chem. Soc., Div. Polym. Chem.)* **2003**, *44* (1), 544.
(20) Birshtein, T. M.; Zhulina, E. B. *Macromol. Theory Simul.* **1997**, *6*, 1169.
(21) Wang, J.-S.; Matyjaszewski, K. *J. Am. Chem. Soc.* **1995**, *117*, 5614.
(22) Matyjaszewski, K.; Xia, J. *Chem. Rev.* **2001**, *101*, 2921.
(23) Matyjaszewski, K. *Chem.—Eur. J.* **1999**, *5*, 3095.
(24) Alexander, S. *J. Phys. (Paris)* **1977**, *38*, 983.
(25) Landau, L. D.; Lifshitz, E. M. *Statistical Physics, Part I*; Pergamon Press: New York, 1970.
(26) Semenov, A. N. *Sov. Phys. JETP* **1985**, *61*, 733.
(27) Stepanyan, R.; Subbotin, A.; ten Brinke, G. *Phys. Rev. E* **2001**, *63*, 061805.
(28) Potemkin, I. I. *Eur. Phys. J. E* **2003**, *12*, 207.

MA021519D